applied sciences

MDPI

Article

Application of Module Ground Clips: An Enhanced and Simplified Approach for PV System Grounding

Jinchel Moon [1,2], Sungmin Woo [1], Seulki Hong [3], Taejun Yun [3], Koo Lee [3] and Myungchin Kim [2,*]

[1] Chungbuk Technopark, Next Generation Energy Center, Yeongudanji-ro 76, Ochang-eup, Chungwon-gu, Cheongju-si 28116, Republic of Korea; jcmoon@cbtp.or.kr (J.M.); ywoosm@cbtp.or.kr (S.W.)
[2] School of Electrical Engineering, Chungbuk National University, 1 Chungdae-ro, Seowon-gu, Cheongju-si 28644, Republic of Korea
[3] Kumkang Electric Industry Co., Ltd., Geumbong-daero 736, Chunju-si 27330, Republic of Korea; nj4050@naver.com (S.H.); dbsxpwns2by64@gmail.com (T.Y.); engine29@naver.com (K.L.)
* Correspondence: mckim@cbnu.ac.kr; Tel.: +82-43-261-3670

Abstract

Recently, the problem of climate change caused by the increase in greenhouse gases has become a major issue, and the importance of eco-friendly energy is increasing worldwide. The installation of PV systems is increasing, and they are being installed in areas adjacent to users. Nevertheless, the concerns relevant to safety problems, such as grounding modules to prevent electric shock accidents, should be addressed. This study examined the effectiveness of applying grounding clips for PV module installations. When the grounding clip was applied, it showed approximately 6.7% improvement compared to the resistance value of the existing grounding wire. The grounding performance and construction convenience of the technology applied with the new grounding clip were verified by a comparison with the existing conventional grounding wire. For manufacturing the clips, a mold with a 32° cone angle and a height of 3.5 mm was used, and a fastening torque of 225 kgf·cm was found to achieve satisfactory grounding resistance values compared to the conventional approach. Using a power tool and expanding it to nine modules (=5.56 kWp), the clip installation process took 585 s, which succeeded in reducing the installation time by approximately 38.1% compared to the 945 s taken using wires. Moreover, the module could be installed and grounded with only a two-step process of installing the module and fastening it with bolts, increasing the installation economy.

Keywords: grounding clip; grounding resistance; photovoltaic (PV)

check for updates

Academic Editor: Maria Vicidomini

Received: 13 September 2025
Revised: 13 October 2025
Accepted: 16 October 2025
Published: 24 October 2025

Citation: Moon, J.; Woo, S.; Hong, S.; Yun, T.; Lee, K.; Kim, M. Application of Module Ground Clips: An Enhanced and Simplified Approach for PV System Grounding. *Appl. Sci.* **2025**, *15*, 11382. https://doi.org/10.3390/app152111382

Copyright: © 2025 by the authors. Licensee MDPI, Basel, Switzerland. This article is an open access article distributed under the terms and conditions of the Creative Commons Attribution (CC BY) license (https://creativecommons.org/licenses/by/4.0/).

1. Introduction

New installed capacity of global solar power in 2024 estimated to be around 599 GW and new global solar power installations are expected to be around 700 GW in 2025, up 17% year-on-year, and about 993 GW will be installed by 2035 [1,2]. While interest in the installation of renewable power sources has shown a continuous increase, about 75% of the overall new renewable installation was performed with PV sources in 2024 [2]. In particular, it is analyzed that the role of solar power generation will increase further as the demand for electricity increases rapidly due to the growth of the electric vehicle and artificial intelligence industries. The AI industry consumes ten times more power than existing search engines, and the demand for solar power will inevitably rise in response to supply [3,4].

The expansion of the supply of PV systems is in a virtuous cycle with the improvement in the economy of PV systems. The economic feasibility of photovoltaics is improving every year, and the supply of PV systems is also increasing rapidly. As the supply of PV systems increases, more user-adjacent systems, such as residential roofs, livestock farm roofs, and BIPV (building-integrated photovoltaics), are being installed, and the safety problems of systems, such as electric shock prevention and module grounding, are greater than ever. Roof-top PV systems are expected to remain stable at approximately 25–30% within the next decade. The construction of BIPV systems and the market share of floating PV plants are also expected to increase gradually [5].

Therefore, with the increase in the installation of large-scale PV power plants, which are eco-friendly and sustainable energy sources, the grounding system is an essential component of the design to ensure compliance with safety and operation guidelines, such as IEC 62548 [6] and KEC (Korean Electrical Code) [7]. A large-scale PV power plant means that the voltage increases in the PV module array. When large-scale PV systems use wire grounding between modules without being grounded to the structure, however, it is probable that the ground wire between the two modules becomes loose as the operation time increases. In such a case, the grounding may become unstable, and the power output could decrease. As the number of PV modules increases, long-term reliability and stability can be secured by performing the grounding between each module and structure in a clip-grounding method in parallel with the bolt fastening method. In large PV systems, however, the leakage current caused by high-voltage systems has been pointed out as one of the important causes of potential difference-induced degradation (PID), which directly affects the performance and life of the PV module [8–10]. PID occurs when there is a high-voltage potential difference between the module and the ground, which reduces the power output and causes problems with the PV system. The impact of PID phenomenon would increase as the potential difference increases. Grounding technology is one important area to prevent this PID problem [11]. In particular, the potential for increased PID risks, which are closely related to grounding technology, would increase as the number of floating PV plants increases. The potential difference also increases as the resistance between the module and ground increases, raising the likelihood of PID occurrence. Although the PID phenomenon is affected also by other factors, such as humidity, temperature, module technology, and operational conditions, grounding is a critical factor in preventing PID and ensuring safe operation of emerging PV systems [12,13]. Therefore, the risk of PV system failures caused by PID could be reduced by applying effective grounding methods between the module frame and the structure.

The PV modules, the balance of system (BOS), and metal structures that make up the PV power plant are connected to the ground by conductor electrodes. A suitable grounding system for each voltage area of a PV power plant provides safety, such as preventing electric shock during system failure and preventing damage to proper insulation in the case of malfunction [14–16]. Although design approaches, guidelines, and considerations for conventional power equipment could also be applied to PV systems, further research on PV system grounding has been performed. For example, the mechanical structures that are commonly used for PV system installation (e.g., panel array foundations and metal support structures) could effectively contribute to grounding similar to auxiliary electrodes [17]. The effects of soil resistivity, grounding system impedance, and fault current characteristics on the PV system grounding were also explored [18]. The performance of various measures, such as dedicated grounding grid, equipotential bonding system (EBD), and lighting rods, for lighting protection was also studied, considering that the transient response of PV systems during lightning events would be affected by the grounding design [19,20]. A hybrid earthing system with zone-specific integration and separation to enhance system

safety while minimizing implementation cost and environmental impact was also proposed. Although such results have been obtained from research on PV grounding systems based on conventional grounding approaches, research on alternative approaches for PV module grounding is limited. Considering that most PV systems are designed or expanded based on the connection of multiple individual PV modules or panels, the grounding and connection approaches applied to PV modules would have a considerable effect on the grounding of the overall PV system [19–24].

In general, PV modules are grounded by assembling a wire or bar-shaped conductor to the module with screws. Therefore, it is common to install the module grounding construction as an additional process after the PV module installation is completed. Although such a conventional approach uses grounding wires for grounding the construction of PV modules, this study incorporated grounding clips into the earthing configuration to reduce the contact resistance between the photovoltaic modules and their frames. The time and cost of the installation process can be reduced by integrating the installation and grounding of the module using a clip-type grounding between the module and the structure. While the wire method is often used for grounding, the risk of screws being separated and resulting in a higher grounding resistance value would rise as the operation time of PV systems increases. In the proposed grounding clip approach, the important points are the spike shape of the clip that connects a grounding without a separate drilling process for making a hole in the PV module frame, and the grounding performance that does not decrease compared to the existing wire method.

The remainder of this paper is structured as follows. Section 2 examines the requirements that the grounding of the PV system should satisfy. Section 3 introduces the design and manufacturing process of the grounding clips. The configuration of the actual grounding clip is shown, and the main design factors are also studied. Section 4 assesses the grounding resistance and the time required to install the proposed approach to determine the effectiveness of the proposed grounding clip. A comparison with the existing grounding wire approach showed that the proposed grounding clip approach realizes effective grounding in an easier and faster installation. The last section concludes the paper.

2. PV System and Grounding Requirements

Figure 1 is a grounding configuration diagram of a PV system consisting of a PV module, a metal structure, and an inverter. Figure 1a presents an overall picture of the grounding in a PV system. Figure 1b shows the grounding between the two PV modules. Figure 1c illustrates the grounding configuration between the structure and the grounding terminal, and Figure 1d shows the connection of the metal structure to the grounding terminal. Figure 1e shows the grounding of the inverter part, which is the exposed conduction part of the PV power plant. The grounding clip covered in this paper is a part applied to the grounding between the two PV modules corresponding to Figure 1b. and the blue circle indicates the grounding part of the photovoltaic systems and indicates parts b, c, d and e.

For most practical installation cases, the PV module grounding process is performed as an additional task after the PV module installation. By applying the grounding clip approach introduced in this paper, however, such a separate module grounding process was not required because the PV module fastening and the grounding processes could be performed simultaneously. In the case of using wires for grounding, changes in the grounding resistance could occur because of the connection being separated or loose. The environmental conditions, such as temperature, humidity, and wind pressure, would also affect the grounding performance. To solve this problem, it is possible to stably maintain ground resistance due to long-term use by fastening the structure and ground between the modules. Meanwhile, the earth ground symbol on the frame of PV modules represents

the part where electricity flows and the metal frame to ensure safety. This is not for the installation of modules, but is only used for the grounding between modules, and is also used for the grounding of the last module and structure of the array. While the ground hole of PV modules can be used, the primary focus of this research is on exploring the safety conditions and effectiveness of the grounding clip approach.



Figure 1. Configuration of PV System Grounding Installation. (**a**) overall picture of the grounding in a PV system; (**b**) module-to-module grounding method; (**c**) module-to-metal structure method; (**d**) metal structure-to-the grounding terminal method; (**e**) grounding of the inverter method.

Although the grounding electrode is generally realized by a buried metal electrode (e.g., copper and aluminum) or the metal structures buried in the ground, the mechanical structures used for installation, such as a steel foundation, are suitable for serving as a grounding electrode in PV systems. Because metal foundations show a relatively low resistance, the overall ground resistance would be determined mostly by the resistance of the soil [19–22]. It is necessary to highlight that concrete, which is used for mounting or supporting the metal foundation, could present a high resistance to the electric current flow. Hence, the effectiveness of the grounding system depends on the size of the grounding resistance, depending on the soil composition, distribution, uniformity, particle size, density, and the concrete foundation.

Figure 2 presents a circuit diagram of the grounding resistance of a PV system composed of one array. In such a case, grounding is performed at five points, and each grounding point corresponds to the grounding point: R_a is the resistance between the solar module frame and the other module frame; R_s is the resistance between two steel structures; R_{s-m} is the resistance between the solar module and the steel structure; R_{s-p} is the resistance between the steel structure and the pole; and R_{ft} represents the footing resistance of the foundation pole.

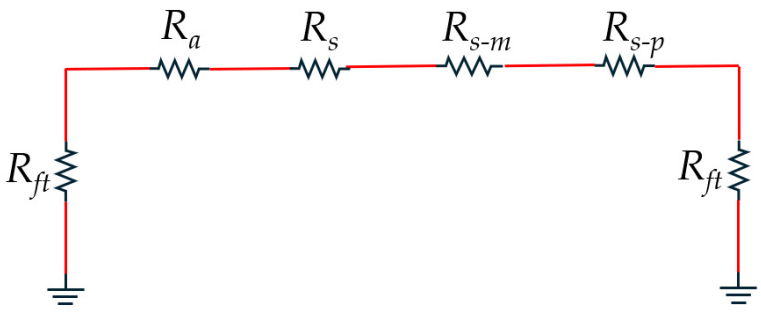


Figure 2. Resistance circuit for the row (PV array).

From the equivalent circuit shown in Figure 2, the grounding resistance of the overall PV system could be expressed as

$$R_{g-PV} = R_{ft} + R_s + R_a + R_{s-m} + R_{s-p} \quad (1)$$

where R_{ft} of a vertical steel structure with a grounding length and diameter of L and d, respectively, could be determined as [21]

$$R_{ft} = \frac{\rho}{2\pi L}\left[\ln\left(\frac{8L}{d}\right) - 1\right] \quad (2)$$

where ρ is the soil resistivity. R_{g_PV} refers to the ground resistance, and according to IEEE 80-141(2000) [25], the ground resistance for transmission and large-scale substations was less than 1 Ω, and the ground resistance range for distribution substations was less than 1 Ω to 5 Ω. The ground resistance affects various aspects of safety, such as the risk of rising ground potential, electric shock risk, lightning strikes, and the inability to disperse increases in fault current.

In the case that the resistance between metal structures and PV module grounding connections is negligible compared to the soil resistance in the ground, R_{g-PV} could be approximated as

$$R_{g-PV} \approx R_{ft} + R_s. \quad (3)$$

approximate Equation (1) by Equation (3) to maintain, the metal structures connected by welding or bolt fastening and the grounding connection between the PV module and the module or the grounding performance between the module and the structure are important [6,25].

Assuming an array composed of infinitely long photovoltaic (PV) structures, as shown in Figure 2, the equivalent resistance can be represented, as shown in Figure 3. In Figure 3, R_{inf} is the equivalent resistance of the long PV array seen from the end of a PV array and can be expressed as [14]

$$R_{inf} = \frac{R_s}{2} + \sqrt{R_s R_{ft}}. \quad (4)$$

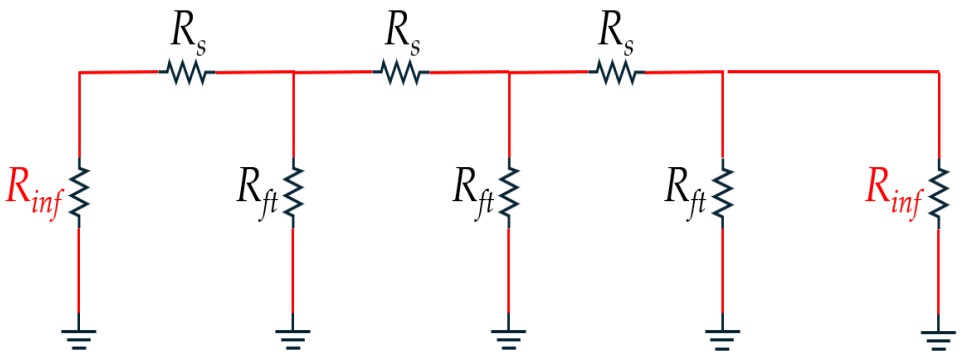


Figure 3. Circuit analysis for the long row (=Long array).

Figure 4 shows that the characteristics of the input ground resistance R_{inf} of an infinite array increases nonlinearly as the soil resistance (ρ) increases. In high-resistance soil, conventional buried ground rods alone are difficult to meet the reference ground resistance. Solar structures are used as auxiliary ground electrodes to overcome these limitations.

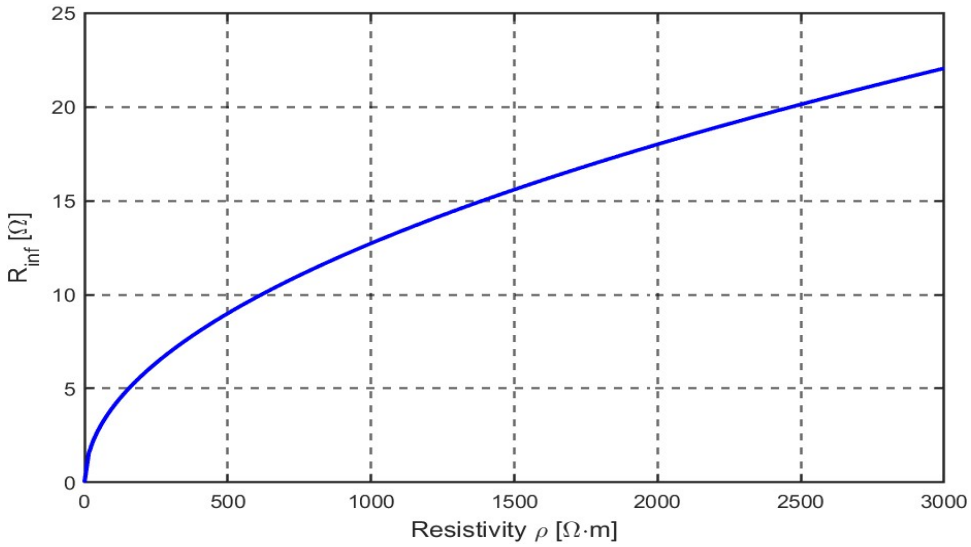


Figure 4. Infinite input resistance for a long infinite row.

According to Barbon et al. [14,15], an effective ground design can be implemented without the embedding of separate electrodes by considering the metal parts of the PV module support structure as auxiliary ground electrodes. On the other hand, there is a limit to ensuring complete electrical continuity with the structure alone. At this time, the ground clip plays an important role. The ground clip allows the structure to function as a practical ground structure by implementing the grounding clips in such a way that the electrical connection between the PV module and the frame is drilled through the surface oxide film to secure conduction between the structures. The application of these grounding clips guarantees the equal potential between modules and also contributes to the reduction in electromagnetic interference [16].

Grounding equipment shall be grounded underground in accordance with the electrical equipment technical standards to protect human life and property from electric shock accidents and fires caused by short circuits. In this study, the requirements defined by KEC (Korean Electrical Code) clause 140-4, which refers to the technical standards and safety requirements for PV systems smaller than 140 kW, were considered. Table 1 lists the requirements for the required type of grounding and ground resistance value depending on the classification of mechanical instruments defined by the KEC. It should be noted that the KEC 140-4 [7]. was established to ensure compliance to standards of IEC 60364-5-54 [26] and IEC 62458 [6]. Effective as of year 2022, KEC was revised to meet the international standards instead of the previous domestic standards [7]. Type 1 grounding is the grounding of components such as metal structures and enclosures for high-voltage and extra-high-voltage electric devices. Type 2 grounding is the grounding of the neutral point or terminal of the transformer that combines the high-voltage and extra-high-voltage electrical lines and the low-voltage electrical line. Type 3 grounding is for the components, such as a metal structure and an outer box of a low-voltage electromechanical device equal to or less than 400 VDC. Type 3 grounding is the connection of the metal structure and outer box of the low-pressure electromechanical device exceeding 400 VDC. In addition, a special Type 3 grounding construction is performed, even if the output voltage of the array exceeds 400 VDC.

Table 1. Types of grounding for the classification of mechanical instruments [7].

Classification of Mechanical Instruments	Types of Grounding	Grounding Resistance Value
For low voltages < 300 VDC	Type 2 grounding	≤150 Ω
For low voltages < 400 VDC	Type 3 grounding	≤100 Ω
400 VDC ≤ For low voltages < 1500 VDC	Special Type 3 grounding	≤10 Ω
1500 VDC ≤ For high voltages ≤ 7000 VDC For extra-high voltage > 7000 VDC	Type 1 grounding	≤10 Ω

In particular, the grounding performance of the PV module is closely related to the safety of a PV power plant; the maximum resistance value is strictly set by classifying the types of grounding. The resistances presented in the table below are the minimum values for safety and are generally much smaller [17,18]. The maximum criterion for the resistance value of the grounding clip to be applied in this paper can be determined using the table above. As suggested in the table above, the grounding clip between the PV modules should secure grounding performance so that the maximum resistance of ≤10 Ω can be measured, even in a high-voltage system.

Table 2 lists the types and specifications used as a grounding electrode. The following data were extracted from the criteria for judging the technical standards of the Electrical Installation Guide 1445 by KEC. The thickness of the grounding line for special Type 3 grounding shall be thicker than or equal to the soft copper wire or equivalent quality and thickness of satisfying ≥2.5 mm^2. The grounding wire should be determined in consideration of regulations and safety, mechanical strength, and corrosion resistance.

Table 2. Grounding wire thickness for Type 3 or Special Type 3 grounding works.

Capacity of Minimum Rated Current	Minimum Thickness of Grounding Wire (Cu, mm^2)	Minimum Thickness of Grounding Wire (Al, mm^2)
≤20 A	2.5	2.5
≤30 A	2.5	2.5
≤50 A	4	4
≤100 A	6	8

Electric shock and electric fire caused by a short circuit can be prevented by grounding the equipment of a PV power plant, referring to the above specifications. This study used crystalline PV modules of the 620 Wp series manufactured by Q-cell. Although Table 3 provides the electrical specification of a single module, the grounding design was performed for a PV generation system with nine PV modules connected in series.

Table 3. Electrical specification of a PV module.

	P_{mp} [W]	I_{sc} [A]	V_{oc} [V]	I_{mp} [A]	V_{mp} [V]	η [%]
STC (Standard Test Condition)	620	13.76	56.67	13.05	47.50	≥22.2
STC of Bifacial Solar Module	654.5	14.54	56.79	13.10	47.50	-

As the maximum voltage of the system was in the range of 400 V < Vsys < 1500 V and a maximum series fuse rating of 30 A was considered for the design, the specification values of Table 3 were used to determine the grounding type (Table 1) and the requirement of the grounding resistance and the minimum thickness of the grounding wire. Therefore, Type 3 grounding or special Type 3 grounding work should be performed. In which case, the thickness (a) of the grounding conductor should be $a \geq$ of 2.5 mm^2 and the grounding resistance (r) should be $r \leq 10$ Ω, as shown in Tables 1 and 2.

3. Design and Manufacturing

3.1. Grounding Clip Configuration

Figure 5 shows several grounding materials commonly used to ground PV modules. Figure 5a shows a copper material and tinned copper braided flexible wire that screw into the frame through holes at both ends. Figure 5b presents the grounding bar of the plated copper material, and Figure 5c shows the grounding wire of the most generally used PV module, which is screw-fixed through terminals at both ends. Figure 5d illustrates the grounding clip used in this experiment, and it was processed by stacking 3 mm thick insulating rubber, a 1 mm thick aluminum plate, and a 0.3 mm thick copper plate. While the aluminum and copper plates were laminated and processed, high-strength carbon steel was used as the lower material.

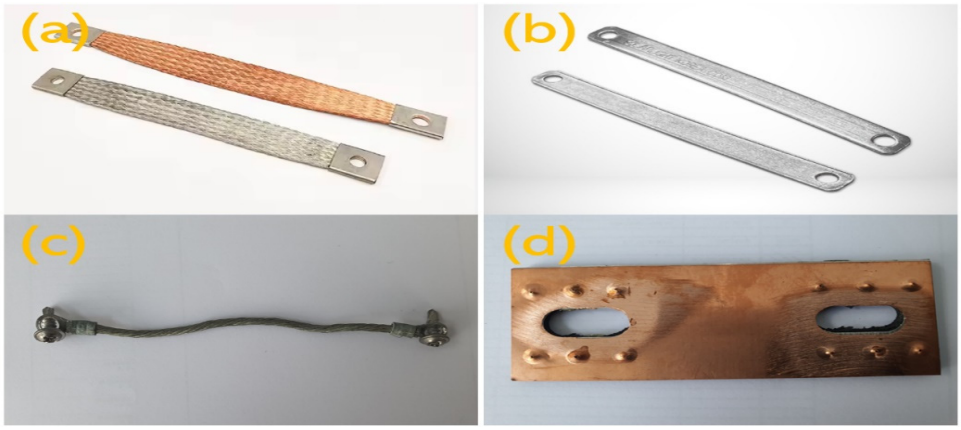


Figure 5. Various types of grounding wires for connecting PV modules. (**a**) a copper material and tinned copper braided flexible wire; (**b**) the grounding bar of the plated copper material (**c**) the grounding wire of the most generally used PV module; (**d**) grounding clip used in this experiment.

Figure 5a–c are in the form of being fastened to the frame of the PV module through a screw. A different clip, Figure 5d, was fastened by the attachment hole of the PV module and installed as an insert between the metal structure and the PV module.

The clip method in Figure 5d applied in this paper can reduce the installation process and time because, unlike other screw methods, such as Figure 5a–c, a separate hole for grounding in the aluminum frame of the PV module is not needed. On the other hand, a separate structure is required to perforate a thin anodizing layer, which is a corrosion-resistant layer of the aluminum frame. Aluminum anodizing is a metal surface treatment technique, which is the process of coating a thin layer of a uniform thickness with aluminum oxide. Anodizing is a process of reinforcing the ductility of aluminum and improving the functional properties, such as corrosion resistance and abrasion resistance, to form a uniform layer with a thickness of approximately 20–100 μm. This layer generally has low conductivity. Hence, the penetrating spikes through the anodizing layer are required for grounding. It is important to penetrate this anodizing layer and contact the conductor with the pure aluminum layer behind it for a grounding connection.

Processing the shape shown in Figure 5d requires a mold with a hydraulic press for elongated elliptical hole processing and spike processing around the hole. A mold capable of hole-perforating and spike processing is needed to mass-produce grounding clips. In this experiment, however, it is more important to understand the factors that determine the spike shape, so a manual mold was used.

Figure 6 presents the procedure of press-processing the grounding clip with a mold equipped with a hydraulic cylinder. Figure 6a shows a picture confirming the dimensions of each part for the press mold, and Figure 6b presents a mill pin applied for processing

the spike for drilling the anodizing film layer. A mill pin generally refers to a pin made by rolling steel. Mill pins are made of various materials and SK-3 grade Ø = 2 mm was applied as the mill pin material in this experiment. The SK-3-grade mill pin is a high-strength carbon steel with excellent wear resistance and easy heat treatment. Figure 6c outlines the process of forming a spike in a clip hole-processed with a mill pin, and Figure 6d shows the aluminum clip processed through the press Figure 6c. The grounding clip used in this experiment is stacked with aluminum and copper plates because the spikes on the clip do not have sufficient strength to penetrate the anodizing film of the aluminum frame of the PV module if it is composed of only a 0.3 mm-thick copper plate. Materials used in clip assemblies (such as copper and aluminum) can cause galvanic corrosion in the long run, increasing ground resistance. Therefore, long-term behavior needs to be monitored.



Figure 6. Machining process of the grounding clamp. (**a**) mold dimension process; (**b**) mill pin applied for processing the spike; (**c**) stacking process with aluminum and copper plates; (**d**) final process grounding clip.

3.2. Spike Processing

Figure 7 presents the name of the cone formation angle and cylinder height of the mill pin in the mold for spike press processing of the grounding clip. Figure 7a shows a mold and a processing protrusion of cone shape for spike processing. It was inserted between the aluminum layer of the clip and the mold such that the 3 mm-thick rubber plate would act as a smooth separation and buffer between the mold and the clip. Figure 7b shows the names of each part of the processing protrusion in the mold for manufacturing the clip. The mill pin is processed into a cone shape for spike processing, where the angle of the cone is θ; the length of the cone is l_1, and the height of the cylinder under the cone is l_2. The cone molding angle θ of the processing protrusion must be processed between 30° and 35° based on the experience value. The angle should be selected so that a complete drilling and embossing process can be performed to produce a gentle protrusion. In the case of $\theta > 35°$, the sharpness of the spikes would be lowered, so the workability of the spike is deteriorated. The length of the cone becomes too large at an acute angle below 35°, so that the spike is perforated, and an appropriate spike shape is not derived. Table 4 lists the results for the angle of the mill pin cone (θ), the length of the cone (l_1), and the height of the cylinder (l_2) under the cone.

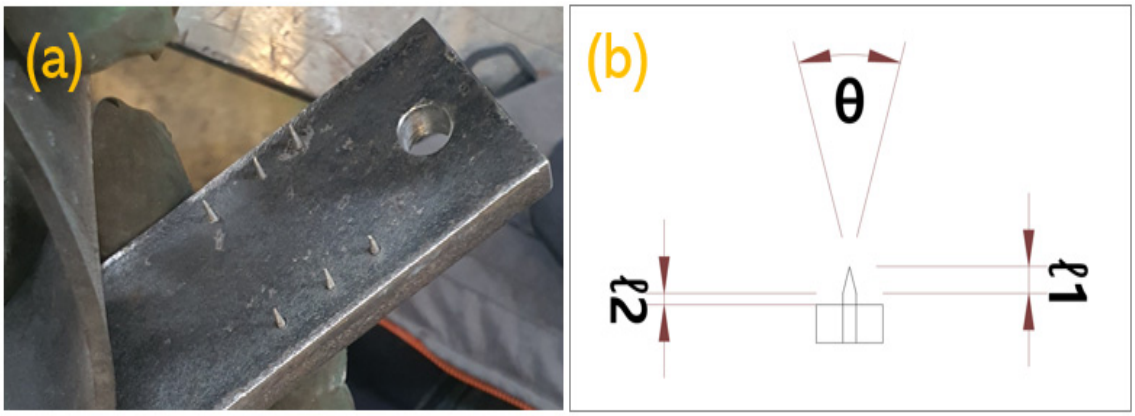


Figure 7. Spike processing mold (mill pin mold). (**a**) spike processing; (**b**) spike design.

Table 4. Height and angle of cone and cylinder.

Item	30°	31°	32°	33°	34°	35°
ℓ_1 (mm)	3.7	3.6	3.5	3.4	3.3	3.2
ℓ_2 (mm)	1.3	1.4	1.5	1.6	1.7	1.8
Total (mm)	5.0	5.0	5.0	5.0	5.0	5.0

In the spike processing mold, the sum height of the processing protrusions combined with the cone and the cylinder was made equal to 5.0 mm in all cases. The thickness of the rubber plate during processing was 3.0 mm, as previously mentioned, and the thickness of the aluminum plate was 1.0 mm. The height of the cone was calculated assuming the rubber plate was not shrunk by compression because the thickness of the copper plate was 0.3 mm. The height of the spike was calculated to be $5.0 - (3.0 + 1.0 + 0.3) = 0.7$ mm.

Figure 8a–f present the angular heights of the cones. Table 5 lists the height and angle of the cone and cylinder for Figure 8. Figure 9 shows the height of the cone and the cylinder according to the mill pin angle for spike processing in the mold presented in Table 5 and Figure 8. Figure 10 shows the spike shape of the press-processed aluminum plate according to the angle presented in Table 4. What is important is the height and shape of the spikes. Figure 10a shows the shape of the pressed spike when the angle of the cone in the mold was 30° and the height was 3.7 mm. The mill pin mold perforated the aluminum plate, and the spike shape was barely made. Figure 10b presents the shape when the angle and height were 31° and 3.6 mm, respectively. Figure 10c shows the shape of the spike when the angle and height were 32° and 3.5 mm, respectively. Figure 10d shows the shape of a spike when the angle and height of the mold cone were 33° and 3.5 mm, respectively, and Figure 10e,f show the shape of a spike when they were 34° and 35°, respectively. As shown in Figure 10, the mold does not work correctly under mold conditions at an angle of 30°, and the aluminum plate was perforated completely.

Table 5. Height of cone and cylinder according to spike angle.

Item	30°	31°	32°	33°	34°	35°
ℓ_1 (mm)	3.7	3.6	3.5	3.4	3.3	3.2
ℓ_2 (mm)	1.3	1.4	1.5	1.6	1.7	1.8
Result	×	△	◯	◯	△	×

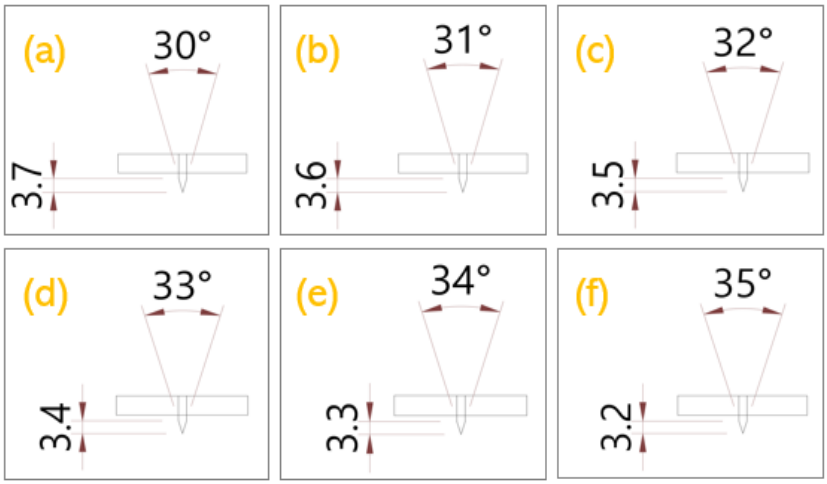


Figure 8. Height of the cone according to the angle. (**a**) Angle 30°, Hight 3.7 mm; (**b**) Angle 31°, Hight 3.6 mm; (**c**) Angle 32°, Hight 3.5 mm; (**d**) Angle 33°, Hight 3.4 mm; (**e**) Angle 34°, Hight 3.3 mm; (**f**) Angle 35°, Hight 3.2 mm.

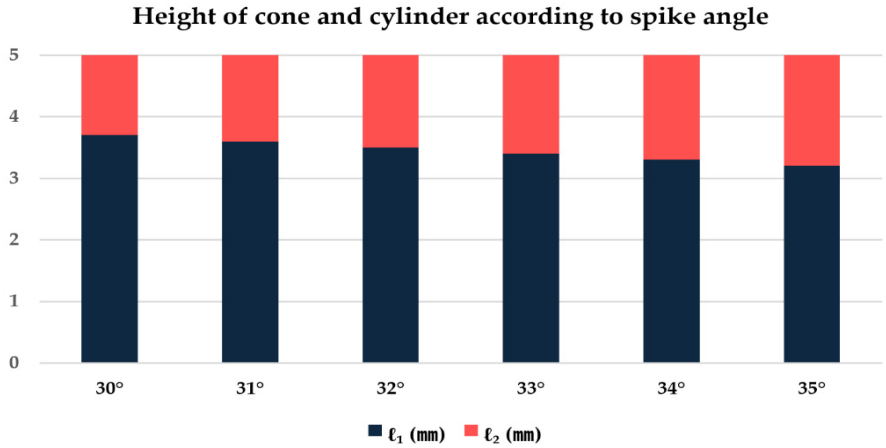


Figure 9. Height of the cone and cylinder according to the spike angle.

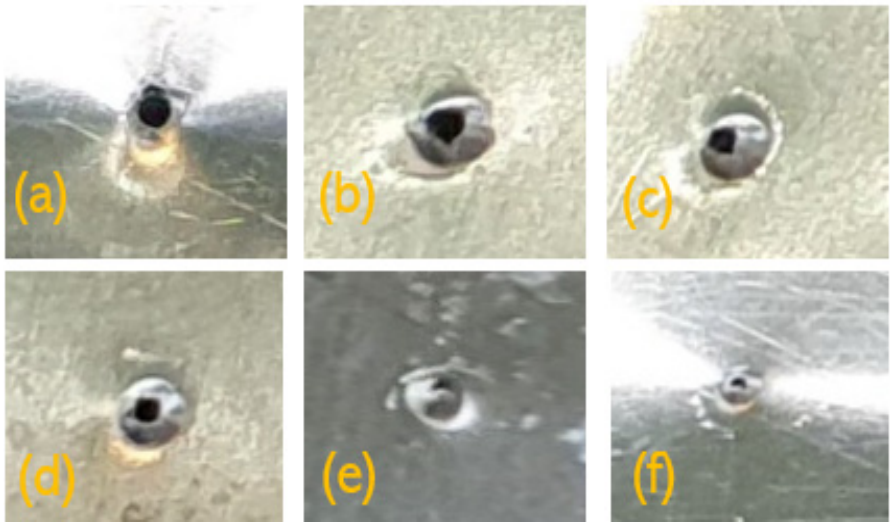


Figure 10. Spike shape pressed according to the angle. (**a**) Angle 30°, Hight 3.7 mm; (**b**) Angle 31°, Hight 3.6 mm; (**c**) Angle 32°, Hight 3.5 mm; (**d**) Angle 33°, Hight 3.4 mm; (**e**) Angle 34°, Hight 3.3 mm; (**f**) Angle 35°, Hight 3.2 mm.

In this case, perforation may also occur in the copper plate located on the upper side of the aluminum plate, and after the press process, the plate is stuck in the mold, resulting in poor productivity. Figure 10b is better than Figure 10a, but the hole is also too large, and the height of the spike is too high, so the spike strength is relatively weak. Even in this case, the spike is not formed properly in the copper plate. Figure 10c,d show the best shape of the spike among the press samples. Figure 10e,f show that the height of the spike was too low, and the sharpness too low, to show the spike shape of the copper plate, and it is difficult to penetrate the anodizing coating layer of the PV module frame. Table 4 summarizes these results. and Table 5 shows the spoke shape and height of the press-processed Al-plate according to the angle, and the results are indicated as good(○), normal(△), and defective or poor(×).

According to the results of Table 5 above, Figure 11 shows the results obtained by pressing the mill-pin-processing protrusion with the cone molding angle $\theta = 32°$, the height of the cone (l_1) = 3.5 mm, and the height of the cylinder (l_2) = 1.56 mm.

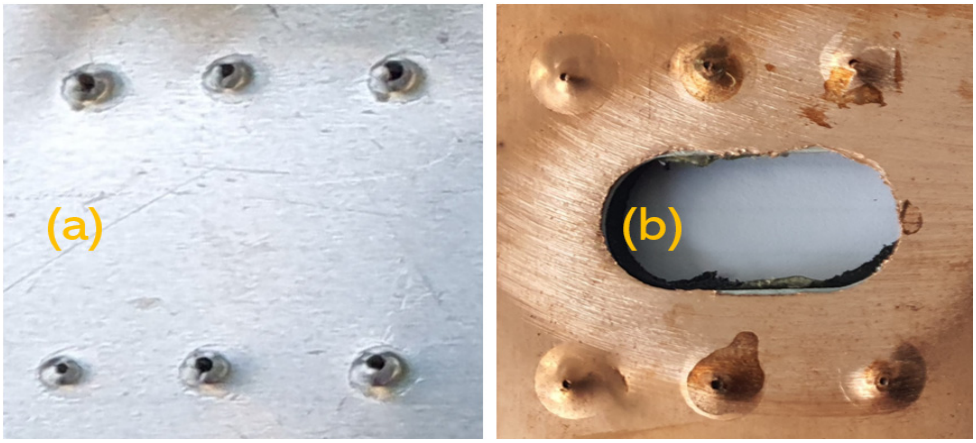


Figure 11. Spike shape pressed by angle: (**a**) Aluminum plate; (**b**) Copper plate.

Figure 11a is the shape of a spike formed by press molding on an aluminum plate, and the spike was not completely perforated. The height of the spike is good and protrudes to an appropriate size. Nevertheless, some of the spikes have a small shape, but there was little deviation on the copper plate. Therefore, there will be no major problem even if the press process is performed at a cone angle of 33°. By contrast, 31° and 34° are somewhat less effective and not recommended because mass productivity is expected to decrease at angles beyond that range. Figure 11b shows the shape of the spike completed by laminating a copper plate above it. The cone shape of the female mold is alive because the copper plate is as thin as 0.3 mm.

3.3. Application of the Grounding Clip

Figure 12 shows the configuration of the grounding clip proposed in this study and the PV module grounding using the conventional grounding wire. Figure 12a shows the use of the grounding clip for PV module grounding. As shown in the figure, the PV module is generally fixed to the C-channel of the structure using bolts and nuts, and the grounding clip enters between the PV module and the metal structure at this part. Therefore, a separate additional fastening device is not required, and a grounding connection is completed at the same time as the PV module is fastened to the structure. Nevertheless, because it is inserted between the structure and the frame of the anodizing layer-treated PV module without drilling an additional fastening hole, a disadvantage exists in that the grounding between PV modules can be completed only when the anodizing layer of the PV module, which is an insulating material, is penetrated. Therefore, in this case, it is essential to check

how much torque should be fastened to penetrate the anodizing layer, and it is essential to confirm that the grounding performance of the module does not deteriorate compared to the previous one.

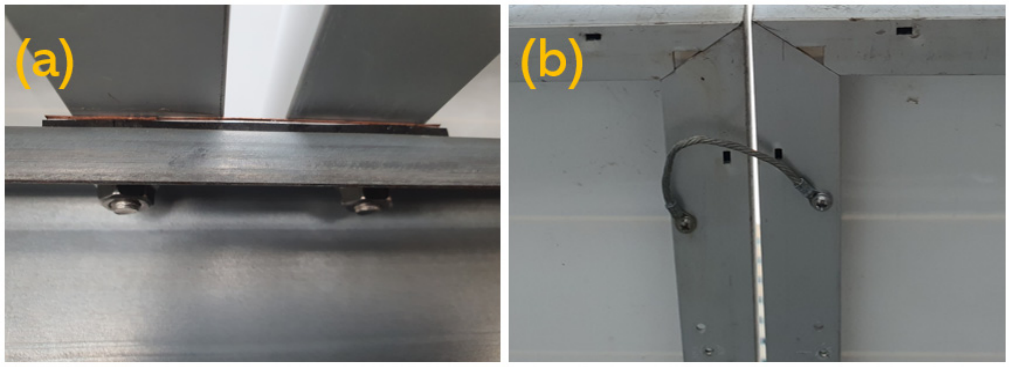


Figure 12. (**a**) module grounding clip and (**b**) grounding wire connecting method.

Figure 12b shows the grounding work between PV modules through the existing grounding wire. This method can secure the grounding performance completely because the grounding cable is connected through the anodizing layer more reliably. On the other hand, the cost can be increased by the additional installation process on the site because the module grounding process must be added collectively after module installation of the structure. Therefore, this study aimed to reduce the cost by processing module grounding in the same way as Figure 12a while having better performance than when module grounding is connected in the way shown in Figure 12b.

The grounding performance of the PV module was compared by measuring the resistance with a resistance meter at both ends of the array of modules connected in series. The resistance should be significantly lower than the 10 Ω suggested in Table 1.

4. Evaluation Results

4.1. Grounding Resistance

The grounding resistances for the conventional and the proposed grounding clip approaches were measured as follows. Figure 13a shows the resistance meter (manufactured by Tynsley) used in this study. The measurement range was 0.1 μΩ to 1, which can accurately measure even very low resistance. Accuracy presents ±1% reliability of the reads from 50 μΩ to 1 Ω, and the user can set a test duration from 15 to 120 s for test currents ranging from 5 A to 200 A. Figure 13b presents a torque wrench manufactured by Tohinichi; the measurable range was 100.6 kgf·cm to 503.8 kgf·cm.

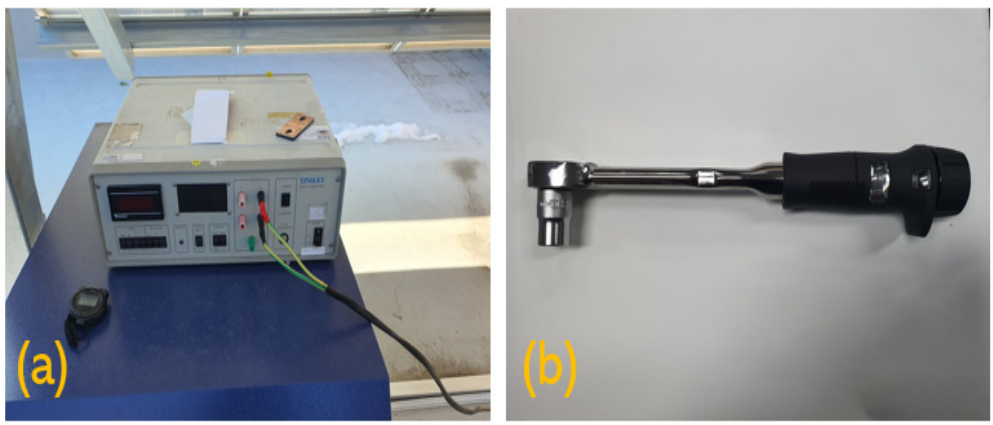


Figure 13. Measurement Equipment: (**a**) resistance meter; (**b**) torque wrench.

Figure 14 presents the process performed for measuring the grounding resistance of the conventional approach. Figure 14a shows the configuration of the grounding wire approach. Figure 14b,c shows the unscrewing of one of the grounding wires connected continuously from both ends in the next array, and connecting them with conductive clamps to the Channels 1 (C1) and 2 (C2) terminals of the resistance meter, respectively. Figure 14d confirms that the cable from Figure 14b is connected to the C1 terminal and the cable from Figure 14c is connected to the C2 terminal. Figure 14a shows the grounding wire, which is commonly used for grounding between PV modules, being assembled by drilling the frame of the PV module using screws and power tools. In this process, a hole is drilled in the module frame using a screw and a power tool, as shown in the figure. In this process, the anodizing layer, which acts as an insulating layer outside the aluminum frame, is destroyed. Subsequently, the PV module grounding circuit is completed by connecting to the grounding cable through the conductor's stainless steel screw and the aluminum terminal. The thickness of the grounding wire was 4 mm^2. As discussed in Section 2, the measured grounding resistance of the PV system should be less than 10 Ω; the actual measured resistance was 16.3 mΩ. As a result, the grounding performance of the reference PV array implemented by applying the existing grounding wire was sufficient.



Figure 14. Resistance test for the grounding wire type. (**a**) connect ground wire; (**b**) Ground measurement terminal connection; (**c**) Measurement of ground resistance; (**d**) grounding resistance measurement result.

Figure 15 shows the process for measuring the grounding resistance of the proposed grounding clip approach. Figure 15a presents the process for separating the existing grounding wire connected in the reference array. Figure 15b outlines the process of releasing previously fixed bolts and nuts to insert a grounding clip between the PV module and the structure. Figure 15c shows the process of inserting a grounding clip between the PV module and structure. When installing at a new site, it is better to attach the grounding clip to the C-channel of the structure in advance. Figure 15d presents the process of assembling the inserted clip with a torque wrench using a module fastening bolt and nut.

The grounding clip method is not a drilling method using a screw. The grounding resistance varies according to the torque because the spike in the clip must penetrate the anodizing layer of the aluminum frame while increasing the torque of the wrench. Considering the effect of torque on the grounding resistance, the relationship between the torque and the grounding resistance was studied, as shown in Figure 16. For each torque level, the grounding resistance was measured five times, and the measurement results are shown in Table 6. From such data, it could be seen that differences among the maximum,

minimum and average values seem to be rather minimal. Among the overall data, the maximum value of the grounding resistance was used for plotting Figure 16.



Figure 15. Measurement of the resistance using the grounding clip connection method. (**a**) Disconnect existing ground wire; (**b**) Insert ground clip between module and structure; (**c**) Insert the ground clip between the disconnected module and the structure; (**d**) the process of assembling with a torque wrench.

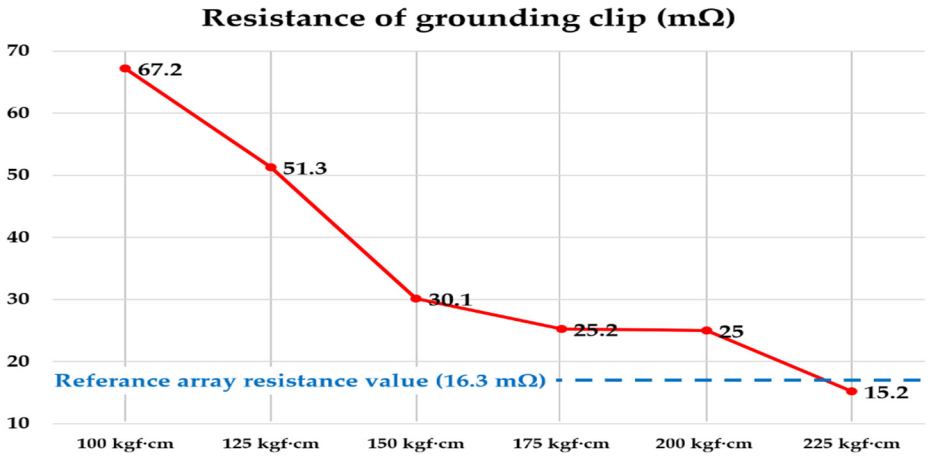


Figure 16. Resistance test result of the grounding clip.

Table 6. Grounding resistance value according to torque pressure (units: mΩ).

Torque Pressure (kgf·cm)	#1	#2	#3	#4	#5	Max.	Min.	Average
100	67.1	67.2	67.1	66.9	67.0	67.2	66.9	67.06
125	51.3	51.2	51.3	51.2	51.1	51.3	51.1	51.22
150	30.1	30.0	30.0	30.1	29.9	30.1	29.9	30.02
175	25.1	25.2	25.1	25.1	25.2	25.2	25.1	25.14
200	24.8	24.8	25	24.9	24.9	25	24.8	24.88
225	15.1	15.2	15.2	15.2	15.1	15.2	15.1	15.16

When a torque of 100 kgf.cm and 125 kgf.cm was applied, the measured grounding resistance was 67.2 mΩ and 51.3 mΩ, respectively. Both cases were lower than the minimum standards presented in Table 2, but the measured resistance was too high compared to the reference value, 16.3 mΩ, which is the value when conventional grounding wire is used. A high resistance means a low grounding performance. This is a result of the grounding clip

being unable to sufficiently penetrate the anodizing layer compared to the conventional screw of the grounding wire. Therefore, the grounding resistance should be measured continuously after adjusting to a higher torque to reach the conductive aluminum layer of the PV module frame. The measured resistance was 30.1 mΩ when a torque of 150 kgf.cm was applied. Such a value was less than half of the 67.2 mΩ measured at 100 kgf·cm torque, but was approximately 184.7% higher than the resistance with the conventional grounding wire applied.

The measured resistance was 25.2 mΩ when a torque of 175 kgf·cm was applied, which did not decrease significantly as before. This is because the cross-sectional area of the existing ground wire was 4 mm^2, and the cross-sectional area of the grounding clip applied in this experiment was 6 mm^2, even if it is based on the narrowest place. Therefore, the cross-sectional area of the conductor is wider, but the high resistance means that the spike of the grounding clip cannot penetrate the anodizing layer of the aluminum frame at this torque level. The other conditions among the resistance components constituting the grounding resistance were the same because the common reference PV array was used. The only difference would be the cross-sectional area of the grounding conductor and the resistance of the anodizing layer. Moreover, the resistance of the anodizing layer should be considered to have been affected in this case because the cross-sectional area of the grounding conductor is larger than that of the conventional wire. Therefore, the resistance should be measured while increasing the torque of the adjustment wrench until the resistance is lower than the reference value. The point where the resistance was lower means that the insulating layer of the anodizing layer is destroyed, and the torque at this time is the torque to be applied to the work standard when the grounding clip is installed.

When a torque of 200 kgf·cm was applied, the resistance was similar to the case when the applied torque was 175 kgf·cm. This area of the torque appears to resist the insulating layer of the anodizing layer before it is destroyed. This hypothesis can be inferred from the sudden decrease in resistance compared to the trend of strengthening the torque in the next measurement value. The measured resistance was 15.2 mΩ when a torque of 225 kgf·cm was applied, indicating an approximately 6.7% lower resistance than the reference value (16.3 mΩ). The resistance measured under this condition was suddenly lower, and the level was also lower than the reference data. Therefore, the insulation layer of the aluminum anodizing layer might be penetrated by the spike of the grounding clip. While the grounding resistance values of both the conventional grounding wire approach and the proposed grounding clip approach are far below the relevant safety limits, it would be desirable to decrease the grounding resistance as much as possible. The grounding resistance would change from its initial value as the operation time increases and the system experiences actual weather conditions. Hence, efforts for realizing the lowest grounding resistance value would contribute to long-time reliability and minimized maintenance needs.

As shown in the above result, the grounding resistance was measured while increasing the torque to a certain level. In general, the resistance continued to decrease as the torque value increased. In a section in which the decrease in resistance was reduced from 175 kgf·cm to 200 kgf·cm, and the slope suddenly decreased to between 200 kgf·cm and 225 kgf·cm, the anodizing insulating layer was destroyed in this torque range. When the grounding resistance was measured while increasing the torque of the wrench from 100 kgf·cm to 225 kgf·cm, the grounding resistance, which initially fell with a similar slope, stagnated around 25 to 30 mΩ. Subsequently, the resistance fell sharply after reaching the conductive layer through the anodizing layer in the range of 200 to 225 kgf·cm. Finally, the grounding clip achieved a grounding resistance of 15.2 mΩ, showing approximately 6.7% improvement compared to the existing grounding wire. During the measurements,

4.2. Time Required for the Installation Process

As mentioned above, the use of the PV module grounding clip may reduce the time and cost of the PV module installation process by simplifying the grounding process. This experiment was applied in a practically installed photovoltaic power generation facility. Figure 17 presents the overall process of PV module installation and the process of mounting a PV module on a metal structure. This sequence is the process of placing the PV module on the installed metal structure and applies equally to the grounding clip and the wire method. In the grounding clip method, an additional simple process of placing the clip on the C-channel of the structure is required. For the ease of attachment, it may be attached between the insulating rubber of the grounding clip and the C-channel of the structure using an adhesive made of a sealant material. The process of placing the PV module varies depending on the location, but it takes approximately 20 to 30 s per PV module. The time to put the grounding clip on is 10 s per location, including the time to apply the sealant, and two places are needed per module, so 20 s is required. Figure 17b presents the process of fastening the PV module using bolts and nuts. This process has no difference in the grounding clip and grounding wire methods. The installation of a module requires significantly more time when using a power tool or a manual tool. In this experiment, it was fastened using a manual tool: 60 s per PV module was taken because 15 s per location and four locations per module are required. Figure 17c shows the process required only by the grounding wire method, and it is a process of screwing the grounding wire between the two modules. Approximately 30 s per location were required, resulting in approximately 60 s because two locations must be drilled per module. Figure 17d shows the grounding between the C-channel of the structure and the square pipe of the structure. This process is essential for the grounding performance of the total PV system, but it does not include the module grounding process of this experiment. In addition, as it is necessary for both the grounding clip and the grounding wire installation process, the time was not measured separately because it was not directly related to the process simplification focused on in this paper. A comparison test was conducted based on the time to go from the processes in Figure 17a–c, which was required for PV module grounding installation. The time was measured and reflected by one person while performing each process because the installation time may vary depending on the person.

The total module array was calculated based on nine solar modules, which is the scale of the installed test bed, and the result is described in the results and discussion session. Table 7 lists the time required for each solar module according to the installation process.

Table 7. Comparison of the time required for installation per solar module.

Installation Process	Grounding Clip	Grounding Wire
Module mounting	25	25
Clip mounting	20	-
Module fastening	60	60
Wire drilling	-	60
Total (sec/module)	105	145

The module mounting process is the process for placing a PV module on the metal structure, and the clip mounting process is the process of placing a grounding clip on the C-channel of the metal structure. In the grounding clip method, it is better to do this process before the module mounting process. The module fastening process involves fastening a solar module placed on a structure using bolts and nuts. Referring to the results in Figure 16, the fixed torque should be performed at 225 kgf·cm or more, and the use of electric tools can save time. This fastening process applies to the existing grounding wire approach and the proposed grounding clip method; there is no time difference, but

the time required is shortened for electric tools. Hence, the time saved on grounding is increased. Wire drilling is a process applied only to the existing grounding wire method and involves drilling and fixing both ends of the grounding wire to the aluminum frame of the PV module using screws. Figure 18 presents a visualization of the results in Table 7.

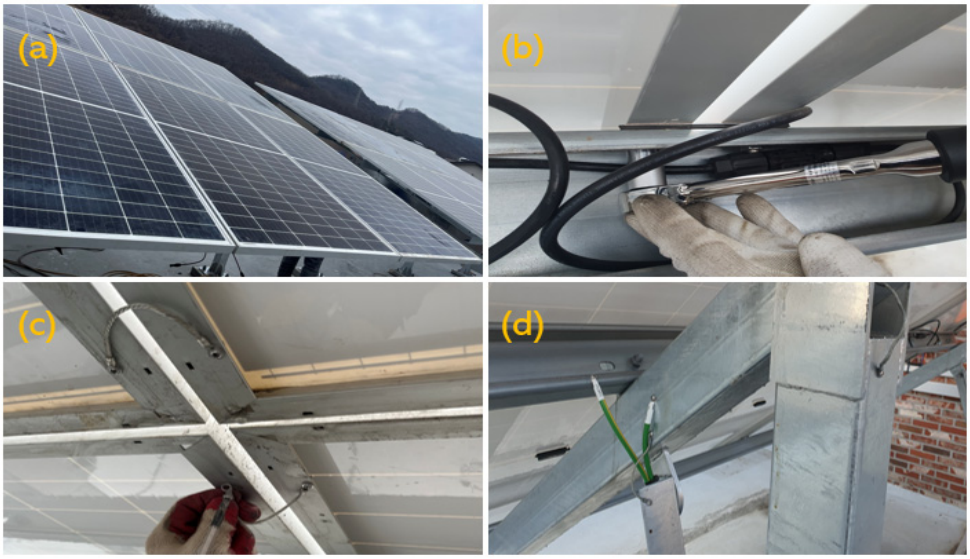


Figure 17. Process of mounting a PV module on a metal structure. (**a**) the process of placing a module on a structure; (**b**) grounding clip method; (**c**) process of screwing the grounding wire between the two modules; (**d**) Grounding Process between Structures and Structures.

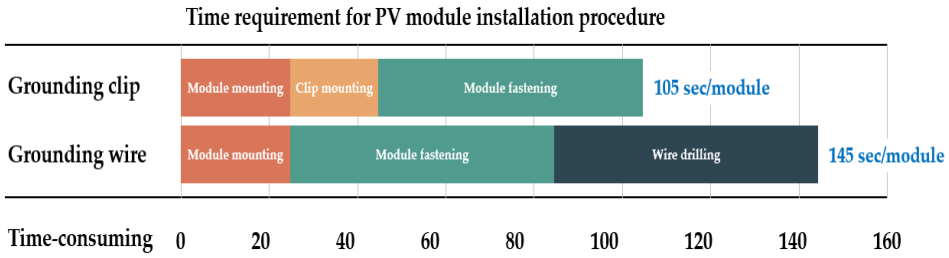


Figure 18. Time requirements for a PV module (single module with hand tools).

As shown in Figure 19, the grounding clip and grounding wire methods have their processes. The clip mounting process is a unique process required only for the grounding clip approach, and the wire drilling process is a distinct process of the wire method. The rest of the process is the same. The difference is determined by the time taken for each unique process. The clip mounting process saves much more time than the wire drilling method, and ultimately reduces the time taken in the entire installation process of the PV module to 105 s vs. 145 s, reducing the installation time by approximately 27.6%.

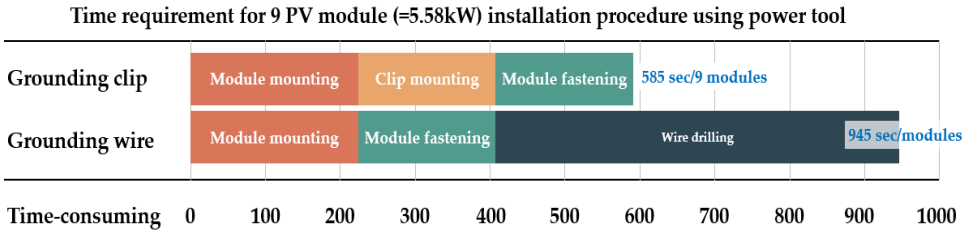


Figure 19. Time requirements for PV modules (nine modules with a power tool).

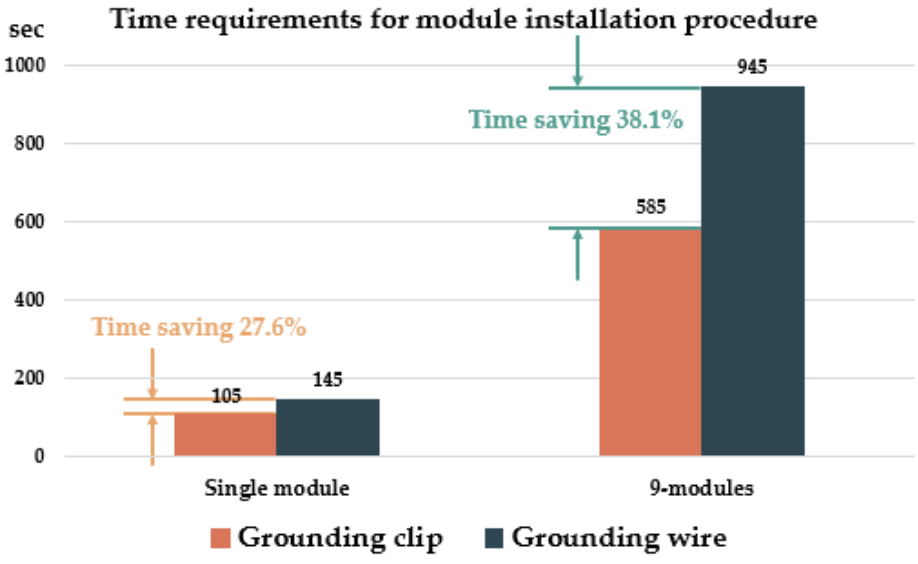
Using power tools, the time spent on PV module fastening can be reduced by one-third compared to using manual tools. The use of a power tool is essential in a system

that requires a large-scale installation of PV modules. The decrease in the cost of the module fastening process increases the dependence of the construction period on the time required for grounding construction in the entire module installation process. The system applied in this paper was a nine-module PV system with a capacity of approximately 5.58 kWp. Table 8 lists the time taken to install a solar module, assuming that these results are converted into the nine-module system (5.58 kWp) and an electric power tool is used for PV module mounting (5 s per location, 20 s per module).

Table 8. Comparison of the time required for the installation of a PV array (nine modules).

Installation Process	Grounding Clip	Grounding Wire
Module mounting	225	225
Clip mounting	180	-
Module fastening	180	180
Wire drilling	-	540
Total (sec/module)	585	945

A comparison of the above results with the manual tool in Table 8 showed that the process required for fastening the module is significantly lower in the entire process. This can be confirmed in the graph, making it easier to distinguish visually, as shown in Figure 20. What the above results mean is that if the installation process becomes large-scale and the power tool is applied to the fastening of the module instead of the hand tool, the importance of grounding clips in the grounding process becomes even greater. According to the experimental results, the time required to install 5.58 kWp of PV modules and grounding was previously 945 s, but the time required to install and ground the PV module was reduced to 585 s when it was changed to a grounding clip, as shown in Figure 19.



Item	Single module	9-modules
Grounding clip	105	585
Grounding wire	145	945

Figure 20. Comparison of the time required for the grounding clip and wire.

The advantages of applying the grounding clip approach instead of the existing grounding wire approach become more evident as the installation capacity of the PV module increases, as shown in Figure 20. As a result, using hand tools in a single module saves 27.6% of the time, while using power tools in nine solar modules increases the time-saving rate to 38.1%. As the size of the solar system increases and the economic feasibility

becomes important, the demand for a reduction in installation costs increases. Therefore, the applicability of the grounding clip is expected to increase.

5. Conclusions

The application impact of the grounding clip method, which can replace the existing grounding wire method, was analyzed to reduce the cost of the PV system and the time required for the grounding construction of the PV module. The requirements on the grounding resistance and thickness of the grounding conductor were derived from technical standards and safety regulations.

The shape of a spike is crucial for the grounding clip to reach the conductive layer by penetrating the anodizing layer on the outer surface of the aluminum frame of the PV module without drilling a hole in the frame. Through several press experiments, the most stable shape of the spike was extruded when the angle of the cone, height of the cone, and height of the lower cylinder were 32°, 3.5 mm, and 1.5 mm, respectively. The resistance of the existing wire ground was measured with different amounts of torque to compare the grounding clip made in this way relative to the existing grounding system composed of wires. Although the grounding resistance decreased as the applied torque increased, a 6.7% improvement was achieved compared to the conventional grounding wire approach when a torque of approximately 200 kgf·cm was applied. The contribution of the proposed grounding clip approach to simplifying and expediting the PV installation process was also studied. A comparison of the time taken to install the ground clip and the module with the existing ground wire showed that it takes 105 s (grounding clip, one-module, and hand tool applied) compared to the 145 s (grounding wire, one-module, and hand tool applied), and the effect of improving the process time by the grounding clip is approximately 27.6%. If this part is applied to the nine solar module systems applied in this paper and calculated to install it as a power tool, the ground clip takes approximately 585 s vs. the ground wire which takes approximately 945 s, finally confirming the improvement in the installation process time by approximately 38.1%. The larger this effect, the larger the number of large-capacity systems, the more the installation of the grounding clip will help reduce the overall construction cost because of the larger module installation capacity.

Safety and economic feasibility are important factors for expanding the supply of PV systems. Incurring more cost or time to increase safety is common. However, in this study, although there is a factor for a very slight increase in material costs, it was offset by an improvement in installation costs, resulting in meaningful results in improving safety and economic feasibility. The experiment's results will serve as a reference for other researchers regarding safety and installation costs. While effectiveness of the proposed grounding clip approach was studied in this paper, future studies are to be performed. In order to evaluate the long-term performance, durability tests under actual conditions such as rain, humidity, and thermal cycles are to be performed. The effect of vibration and mechanical stress is also to be studied with a focus on comparison with the conventional wire grounding approach. In addition, quantitative studies on cost effectiveness of the grounding clip approach compared to the conventional approach are also to be performed as future work.

Author Contributions: Conceptualization, formal analysis, writing—original draft preparation J.M.; conceptualization, formal analysis, S.W.; investigation, data curation, S.H.; sample production, experimental measurement, T.Y.; project administration, K.L.; supervision, project administration, M.K. All authors have read and agreed to the published version of the manuscript.

Funding: This research was supported by grants from the Development of Regional Innovation Clusters Program of the Korea Institute for Advancement of Technology (KIAT) funded by the Korean Ministry of Trade, Industry and Energy (MOTIE) (Project No. P0025344). This research was supported

by the Basic Science Research Program through the National Research Foundation of Korea (NRF) funded by the Ministry of Education (RS-2020-NR049604). In addition, this research was supported by the Regional Innovation System and Education (RISE) program through the (Chungbuk Regional Innovation System and Education Center), funded by the Ministry of Education (MOE) and the (Chungcheongbuk-do), Republic of Korea (2025-RISE-11-014-03).

Data Availability Statement: The data presented in this study are available on request from the corresponding author.

Conflicts of Interest: Authors Seulki Hong, Taejun Yun and Koo Lee were employed by the company Kumkang Electric Industry Co., Ltd. The remaining authors declare that the research was conducted in the absence of any commercial or financial relationships that could be construed as a potential conflict of interest.

References

1. Arruebo, A.; Gorremans, J.; Le Pénuizic, L.; Lits, C.; Rossi, R.; Schmela, M. *1Q Global PV Market Outlook*; BloombergNEF. 4 March 2024. Available online: https://about.bnef.com/insights/clean-energy/1q-2024-global-pv-market-outlook/ (accessed on 12 October 2025).
2. Jouanneau, C.; Denain, M.; Guernion, L.; Bidaud, T.; Kouame, K.; Weiss, M.; Turala, A.; Danovitch, D.; Bryche, J.-F.; Darnon, M.; et al. *Design, Manufacture and Characterization of Compact Optics for Micro-CPV*; EDP Sciences: London, UK, 2025. [CrossRef]
3. Masson, G.; The International Energy Agency (IEA). *A Photovoltaic Power Systems Programme (IEA PVPS), Snapshot of Global PV Markets 2025*; IEA-PVPS: Paris, France, 2025.
4. Aljbour, J.; Wilson, T. Powering Intelligence: Analyzing Artificial Intelligence and Data Center Energy Consumption. EPRI. 2024 White Paper. Available online: https://www.epri.com/research/products/3002028905 (accessed on 12 October 2025).
5. Fischer, M.; Woodhouse, M.; Baliozian, P. International Technology Roadmap for Photovoltaics (ITRPV) 2023 Results, 15. Edition, May 2024. Available online: https://www.vdma.eu/international-technology-roadmap-photovoltaic (accessed on 12 October 2025).
6. *IEC 62548 (2023)*; Photovoltaic (PV) Arrays—Part 1: Design Requirements. International Electrotechnical Commission: Singapore, 2023.
7. *KEC 140-4*; Solar Power Generation Refers to the Technical Standards and Safety Requirements. Korea Electric Association: Seoul, Republic of Korea, 2025. Available online: www.kea.kr (accessed on 12 October 2025).
8. Mahmood, F.I.; TamizhMani, G. Impact of different backsheets and encapsulant types on potential induced degradation (PID) of silicon PV modules. *Sol. Energy* **2023**, *252*, 20–28. [CrossRef]
9. Vishal Puranik, E.; Gupta, R. Novel Quantitative Electroluminescence Method for Detailed Performance Analysis of PID-s Affected Crystalline Silicon PV Module. *IEEE J. Photovolt.* **2021**, *11*, 1470–1478. [CrossRef]
10. Ma, M.; Wang, H.; Xiang, N.; Yun, P.; Wang, H. Fault diagnosis of PID in crystalline silicon photovoltaic modules through I-V curve. *Microelectron. Reliab.* **2021**, *126*, 114236. [CrossRef]
11. Badran, G.; Dhimish, M. Potential Induced Degradation in Photovoltaic Modules: A Review of the Latest Research and Developments. *Solar* **2023**, *3*, 322–346. [CrossRef]
12. Finsterle, T.; Cerna, L.; Hrzina, P.; Rokusek, D.; Benda, V. Diagnostics of PID Early Stage in PV Systems. *Energies* **2021**, *14*, 2155. [CrossRef]
13. Goswami, A.; Sadhu, P.K. Degradation analysis and the impacts on feasibility study of floating solar photovoltaic systems, Sustainable Energy. *Grids Netw.* **2021**, *26*, 100425. [CrossRef]
14. Nassereddine, M.; Ali, K.; Nohra, C. Photovoltaic solar farm: Earthing system design for cost reduction and system compliance. *Int. J. Electr. Comput. Eng.* **2020**, *10*, 2884–2893. [CrossRef]
15. Barbon, A.; Bayon-Cueli, C.; Bayon, L.; Carreira-Fontao, V. A methodology for an optimal design of ground-mounted photovoltaic power plants. *Appl. Energy* **2022**, *314*, 118881. [CrossRef]
16. Kroner, D.; Lundgren, U.; Augusto, A.; Bollen, M. Radiated Electromagnetic Emission from Photovoltaic Systems-Measurement Results: Inverters and Modules. *Energies* **2024**, *17*, 1893. [CrossRef]
17. Datsios, Z.G.; Mikropoulos, P.N. Safe grounding system design for a photovoltaic power station. In Proceedings of the 8th Mediterranean Conference on Power Generation, Transmission, Distribution and Energy Conversion (MEDPOWER 2012), Cagliari, Italy, 1–3 October 2012; IEEE: New York, NY, USA, 2012; pp. 1–6. [CrossRef]
18. Schaerer, R.; Lewis, D. Large utility-scale photovoltaic solar power plant grounding system design-general practices and guidance. In Proceedings of the 2015 IEEE Power & Energy Society General Meeting, Denver, CO, USA, 26–30 July 2015.

19. Zhang, Y.; Li, B.; Du, Y.; Ding, Y.; Cao, J.; Lv, J. Effective Grounding of the Photovoltaic Power Plant Protected by Lightning Rods. *IEEE Trans. Electromagn. Compability* **2021**, *64*, 1128–1136. [CrossRef]
20. Kermani, B.; Shariatinasab, R. Protection of Photovoltaic Systems Against Direct Lightning Strokes. *IEEE Trans. Power Deliv.* **2025**, *40*, 301–313. [CrossRef]
21. Illias, H.A.; Su, C.S.; Bakar, A.A. Investigation on soil resistivity of two-layer soil structures using infinite element analysis method. *IET Sci. Meas. Technol.* **2021**, *15*, 120–129. [CrossRef]
22. Parashar, V.; Mishra, B. Designing efficient soil resistivity measurement technique for agricultural wireless sensor network. *Int. J. Commun. Syst.* **2021**, *34*, e4785. [CrossRef]
23. Zhang, C.; Liao, Y.; Gao, X.; Zhao, J.; Yuan, Y.; Liao, R. Research Advances of Soil Corrosion of Grounding Grids. *Micromachines* **2021**, *12*, 513. [CrossRef] [PubMed]
24. Sinchi, F.; Coronel-Naranjo, C.; Barragan-Escandon, A.; Quizhpi-Palomeque, F. Soil Treatment to Reduce Grounding Resistance by Applying Low-Resistivity Material (LRM) Implemented in Different Grounding Systems Configurations and in Soils with Different Resistivities. *Appl. Sci.* **2022**, *12*, 4788. [CrossRef]
25. *IEEE 80-141*; IEEE (Institute of Electrical and Electronics Engineers) Guide for Safety in AC Substation Grounding. IEEE: New York, NY, USA, 2000. Available online: https://ieeexplore.ieee.org/iel5/6948/18673/00861340.pdf (accessed on 12 October 2025).
26. *IEC 60364-5-54:2011*; Part 5-54: Selection and Erection of Electrical Equipment—Earthing Arrangements and Protective Conductors. International Electrotechnical Commission (IEC): Singapore, 2011. Available online: https://webstore.iec.ch/en/publication/1882 (accessed on 12 October 2025).

Disclaimer/Publisher's Note: The statements, opinions and data contained in all publications are solely those of the individual author(s) and contributor(s) and not of MDPI and/or the editor(s). MDPI and/or the editor(s) disclaim responsibility for any injury to people or property resulting from any ideas, methods, instructions or products referred to in the content.